Inorganic Chemistry

Article

pubs.acs.org/IC

High-Pressure Synthesis of the Cobalt Pyrochlore Oxide $Pb_2Co_2O_7$ with Large Cation Mixed Occupancy

Junye Yang,[†,‡] Jianhong Dai,[†,‡] Zhehong Liu,[†,‡] Runze Yu,[§] Hajime Hojo,[§] Zhiwei Hu,[∥] Tunwen Pi,[⊥] Yunliang Soo,[#] Changqing Jin,[†,‡,&] Masaki Azuma,*[,§] and Youwen Long*[,†,‡,&]

[†]Beijing National Laboratory for Condensed Matter Physics, Institute of Physics, Chinese Academy of Sciences, Beijing 100190, People's Republic of China

[‡]School of Physics, University of Chinese Academy of Sciences, Beijing 100190, People's Republic of China

[§]Laboratory for Materials and Structures, Tokyo Institute of Technology, 4259 Nagatsuta, Midori, Yokohama, 226-8503, Japan

[∥]Max-Planck Institute for Chemical Physics of Solids, Nöthnitzer Straße 40, 01187 Dresden, Germany

[⊥]National Synchrotron Radiation Research Center, 101 Hsin-Ann Road, Hsinchu 30077, Taiwan

[#]Department of Physics, National Tsing Hua University, 101 Section 2 Kuang-Fu Road, Hsinchu 30013, Taiwan

[&]Collaborative Innovation Center of Quantum Matter, Beijing 100190, People's Republic of China

ABSTRACT: The novel $A_2B_2O_7$-type compound $Pb_2Co_2O_7$ was synthesized at 8 GPa and 1673 K. Synchrotron X-ray diffraction shows a cubic pyrochlore structure with space group $Fd\bar{3}m$. Rietveld structural analysis reveals a large cation mixed occupancy at both *A* and *B* sites by about 40%, the greatest value found in the pyrochlore family. In combination with the X-ray absorption spectroscopy results, the specific chemical composition and charge states are determined to be $(Co_{0.6}Pb_{0.4})^{3+}{}_2(Pb_{0.6}Co_{0.4})^{4+}{}_2O_7$, in which both the *A*-site Co^{3+} and the *B*-site Co^{4+} are low-spin. Due to the tetrahedral geometric frustration effects as well as the random Co^{4+} and Pb^{4+} distribution at the *B* site, spin glassy behavior is well observed following the conventional critical slowing down feature in $Pb_2Co_2O_7$.

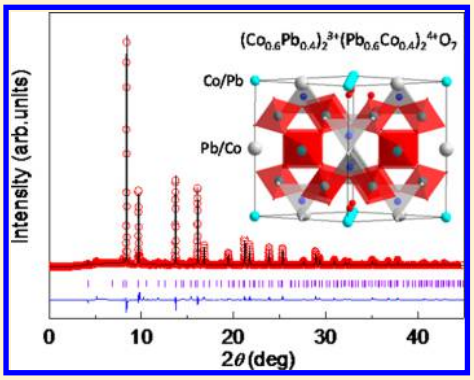

I. INTRODUCTION

Pyrochlore oxides with chemical formula $A_2B_2O_7$ (or $A_2B_2O_6O'$) have been attracting much attention due to their fascinating chemical and physical properties such as superconductivity observed in $Cd_2Re_2O_7$, giant magnetoresistance in $Tl_2Mn_2O_7$, unconventional anomalous Hall effect in metallic $Nd_2Mo_2O_7$, Kondo-like effect in $Pr_2Ir_2O_7$, etc.[1−4] Pyrochlore often crystallizes in a face-centered cubic structure with space group $Fd\bar{3}m$ (No. 227). As shown in Figure 1a, the *A*-site cation in the pyrochlore with larger ionic size occupies the special atomic position 16*d* (1/2, 1/2, 1/2), which is coordinated by eight oxygens (6 O and 2 O′), while the smaller *B*-site cation is located at the special site 16*c* (0, 0, 0) with 6-fold oxygen coordination, forming distorted BO_6 octahedra. The two distinct oxygen positions are at 48*f* (*x*, 1/8, 1/8) for O and 8*b* (3/8, 3/8, 3/8) for O′. Moreover, when one considers the polyhedra composed of the nearest neighboring *A*-site or *B*-site cation, both $O'A_4$ and OB_4 tetrahedra with geometric frustration can form. As a consequence, nontrivial spin properties such as spin liquid and spin ice may occur in pyrochlore oxides.[5]

In past decades, the cobalt oxides have been investigated intensely due to their versatile functional properties. For example, high ferromagnetic Curie temperature is found in $SrCoO_3$ single crystals.[6,7] On the other hand, the oxygen-deficient $SrCoO_{3-\delta}$ shows reversible redox reactions, making it promising for developing highly sensitive electrochemical sensors.[8] The layered $LiCoO_2$ and the double perovskite $(Nd,Ba,Ca)_2Co_2O_{5+\delta}$ have been studied widely in solid oxide fuel cells.[9,10] In addition, a giant magnetoresistance effect is observed in $LnBaCo_2O_{5+\delta}$ (*Ln* = Eu, Gd)[11] and collinear-magnetism-driven ferroelectricity is found in Ca_3CoMnO_6.[12,13] In parallel to the study of Co-based oxides, the Pb-based oxides have also attracted much attention owing to their functional properties such as piezoelectricity, ferroelectricity, and multiferroicity.[14−16] Unfortunately, however, as far as the Pb−Co−O ternary system is concerned, the number of compounds is extremely limited. It appears that the recently discovered perovskite $PbCoO_3$ ($Pb^{2+}Pb^{4+}{}_3Co^{2+}{}_2Co^{3+}{}_2O_{12}$) with both *A*- and *B*-site charge orderings is the only known example of this ternary system to date.[17] In this paper, we report the new finding of the Co-based pyrochlore $Pb_2Co_2O_7$, which can only be stabilized under high-pressure and -temperature conditions probably due to the large cation mixed occupancy at both *A* and *B* sites.

Received: June 28, 2017
Published: September 18, 2017

DOI: 10.1021/acs.inorgchem.7b01646
Inorg. Chem. 2017, 56, 11676−11680

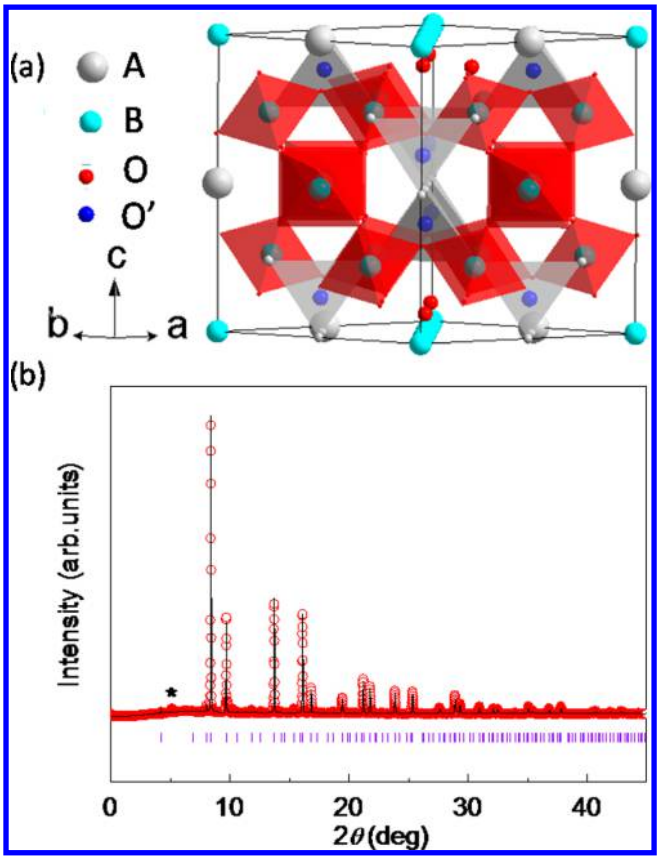

Figure 1. (a) Crystal structure of pyrochlore oxide $A_2B_2O_6O'$ with space group $Fd\bar{3}m$. (b) SXRD pattern collected at room temperature and Rietveld refinement results for $Pb_2Co_2O_7$. Observed (red circle), calculated (black line), and difference (blue line) profiles are shown together with the allowed Bragg reflections (ticks). The asterisk denotes a small amount of an unknown impurity phase (<2%).

II. EXPERIMENTAL DETAILS

Polycrystalline $Pb_2Co_2O_7$ was prepared under high-pressure and high-temperature conditions using a cubic-anvil-type high-pressure apparatus. Highly pure (>99.9%) PbO_2 and CoO powders with a 1:1 mole ratio were used as starting materials. In addition, excess $KClO_4$ was used as an oxidizing agent. These reactants were thoroughly mixed in an agate mortar within an argon-filled glovebox and then sealed into a platinum capsule 2.8 mm in diameter and 4.0 mm in length. The capsule was treated at 8 GPa and 1673 K for 1/2 h. When the heat treatment was finished, the sample was quenched to room temperature, and the pressure was gradually released. The residual KCl in the final product was washed out by deionized water.

Synchrotron X-ray diffraction (SXRD) on powder samples was carried out using a large Debye−Scherrer camera on beamline BL02B2 in SPring-8 with the wavelength λ = 0.4199 Å. The SXRD data were analyzed using the Rietveld refinement program FullProf.[18] The soft X-ray absorption spectroscopy (XAS) at the Co $L_{2,3}$ edges was measured with total electron yield at the BL08B beamline of the National Synchrotron Radiation Research Center (NSRRC) in Taiwan. The hard XAS at the Pb L_3 edges was measured in the transmission geometry at the BL07A beamline of the NSRRC. The temperature-dependent dc magnetic susceptibility (χ_{dc}) and field-dependent isothermal magnetization (M) were measured on a commercial superconducting quantum interference device magnetometer (Quantum Design). The magnetic susceptibility data were collected between 2 and 400 K at different magnetic fields with a temperature sweep model at a rate of 3 K/min. The temperature dependence of ac magnetization (M'), resistivity, and specific heat were measured by using a Quantum Design physical property measurement system.

III. RESULTS AND DISCUSSION

Figure 1b shows the SXRD pattern of $Pb_2Co_2O_7$ measured at room temperature. All of the diffraction peaks can be well indexed on the basis of an $A_2B_2O_7$-type pyrochlore structure model with space group $Fd\bar{3}m$. Since the high-resolution synchrotron X-ray is sensitive enough to distinguish the heavy atoms Pb and Co, the distribution for these two cations was examined by refining the occupancy parameter. When the Pb/Co atoms were constrained to fully occupy the A/B sites or B/A sites, a much higher agreement factor R_p (>30%) was always obtained. In contrast, however, if we refined the occupancy parameter for these two sites by allowing Pb and Co to freely occupy the A or B site, the R_p factor was sharply reduced to a satisfied value of less than 5%. The good agreement between the measurement data and the Rietveld refinement is shown in Figure 1b by considering the Pb/Co free occupancy but constraining the total occupancy factor to be unity for either the A or B site. Note that during the refinement the occupancy factor of oxygen is fixed to unity since the XAS results illustrate the almost stoichiometric oxygen content (discussed later). Table 1 gives the related refined structural parameters. A considerable Pb−Co mixed occupancy is found to occur, i.e. the A site is occupied by about 60% Co and 40% Pb and vice versa for the B site, indicating the detailed chemical composition to be $(Co_{0.6}Pb_{0.4})_2(Pb_{0.6}Co_{0.4})_2O_7$. Although the mixed occupancy effect is also observed in other pyrochlores, the mixed occupancy degree is usually less than 25%.[19] The current $Pb_2Co_2O_7$ thus exhibits the greatest mixed occupancy in the pyrochlore family discovered so far. As shown later, the charge states of Pb and Co at different atomic sites are different to ensure that the A-site average ionic radius is larger than that of the B-site. This distinct charge distribution can effectively prevent the random $A-B$ antisite disorder of cations. In any event, $Pb_2Co_2O_7$ provides the first Co-based oxide possessing a cubic pyrochlore structure.

Table 1. | Crystallographic Parameters of $Pb_2Co_2O_7$ Refined from SXRD Pattern at Room Temperature[a]

atom	site	g	x	y	z	U_{iso} (Å^2)
Co1	16*d*	0.61(7)	0.5	0.5	0.5	0.387(5)
Pb1	16*d*	0.39(4)	0.5	0.5	0.5	0.387(5)
Pb2	16*c*	0.61(7)	0	0	0	0.145(3)
Co2	16*c*	0.39(4)	0	0	0	0.145(3)
O1	48*f*	1	0.3219(2)	0.125	0.125	0.456(3)
O2	8*b*	1	0.375	0.375	0.375	0.515(2)

[a]Crystal data: space group $Fd\bar{3}m$ (No. 227), Z = 8, a = 9.95776(2) Å, ρ_{calc} = 5.0907(1) g/cm^3, V = 987.30(1) Å^3, R_{wp} = 8.9%, R_p = 4.7%. g denotes the occupancy factor.

It is well-known that the multiplet spectral features in the XAS data at the 3d transition-metal $L_{2,3}$ edges are very sensitive to the valence and spin states as well as the local environment.[20,21] To identify the charge and spin states of Co, we performed the Co $L_{2,3}$ XAS measurements. Figure 2a shows the Co $L_{2,3}$ XAS of $Pb_2Co_2O_7$ together with that of $EuCoO_3$ and $BaCoO_3$ used as low-spin Co^{3+} and Co^{4+} references with CoO_6 octahedral coordination, respectively.[20] As shown in Figure 2a, $Pb_2Co_2O_7$ has an XAS profile similar to those of these two references, suggesting the presence of low-

DOI: 10.1021/acs.inorgchem.7b01646
Inorg. Chem. 2017, 56, 11676−11680

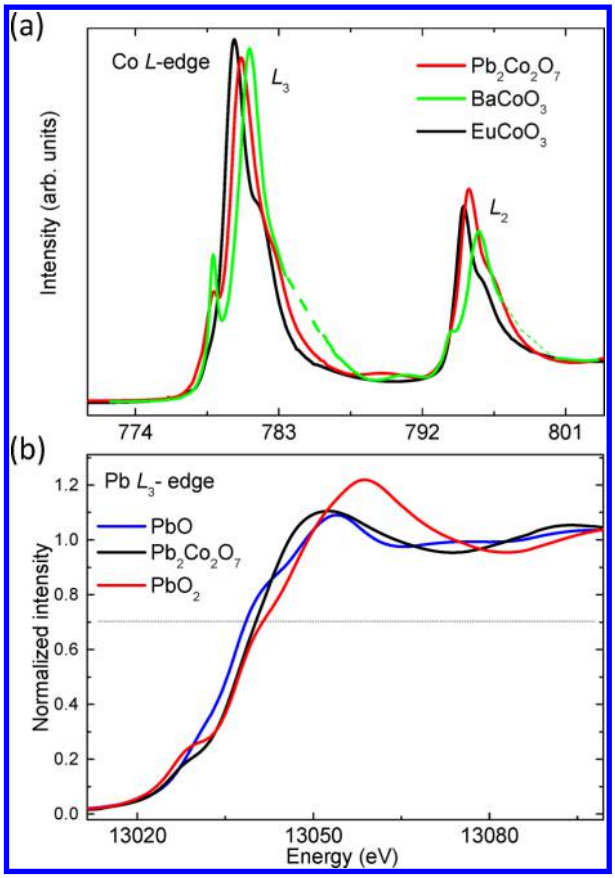

Figure 2. XAS of (a) Co $L_{2,3}$ edges and (b) Pb L_3 edge of $Pb_2Co_2O_7$. The XAS spectra of some related references are also shown for comparison.

spin Co ionic states in $Pb_2Co_2O_7$. Note that the XAS spectral feature of $Pb_2Co_2O_7$ is also similar to that observed in the Co^{3+} and Co^{4+} mixed system Na_xCoO_2, in which low-spin Co ions emerge as well.[20,21] In addition, we find that the absorption spectrum of $Pb_2Co_2O_7$ displays an apparent energy shift relative to the references. For example, the L_3 edge peak position is located at 780.2 eV for $EuCo^{3+}O_3$, 780.6 eV for $Pb_2Co_2O_7$, and 781.2 eV for $BaCo^{4+}O_3$. By comparison, the valence state of Co ions in $Pb_2Co_2O_7$ is determined to be +3.4 on average, suggesting Co^{3+}:Co^{4+} = 3:2 (i.e., $Co^{3+}{}_{1.2}Co^{4+}{}_{0.8}$ in each formula unit). For the hard XAS of the heavier element Pb, the chemical shift of the Pb L_3 edge defined at $\mu \approx 0.7-0.8$ of the normalized intensity can be used to determine the valence state.[22,23] In Figure 2b one can see that the Pb L_3 edge shifts to higher energy from the Pb^{2+} reference PbO to the current $Pb_2Co_2O_7$ and then to the Pb^{4+} reference PbO_2. According to the systematic energy shift of the absorption edge, we estimate a $Pb^{3.6+}$ average valence state in $Pb_2Co_2O_7$. When the structural refinement and XAS results are combined, the detailed chemical and charge formula of $Pb_2Co_2O_7$ can be assigned to be $(Co_{0.6}Pb_{0.4})_2{}^{3+}(Pb_{0.6}Co_{0.4})_2{}^{4+}O_7$, where Co^{3+} and the average Pb^{3+} occupy the pyrochlore *A* site with a mole ratio of 3:2, whereas Pb^{4+} and Co^{4+} occupy the *B* site with an identical ratio. This formula is also in accordance with the charge balance requirement for the stoichiometric oxygen content. Note that Pb is a valence skipper element;[17] therefore, the average Pb^{3+} state occurring at the *A* site should be composed of $Pb^{2+}{}_{0.5}Pb^{4+}{}_{0.5}$ in reality.

As mentioned above, although there exists a large Pb−Co mixed occupancy at both *A* and *B* sites, the *A*−*B* intersite disorder can be reduced significantly by the distinct charge states and ionic sizes of these two cations at different atomic sites. Moreover, both the *A*-site Co^{3+} and the *B*-site Co^{4+} are low-spin in nature. This means that the Co^{3+} is nonmagnetic and insulating. As a consequence, the magnetism and electrical transport will be dominated by the corner-sharing BO_6 octahedra in the current $Pb_2Co_2O_7$. Figure 3 presents the

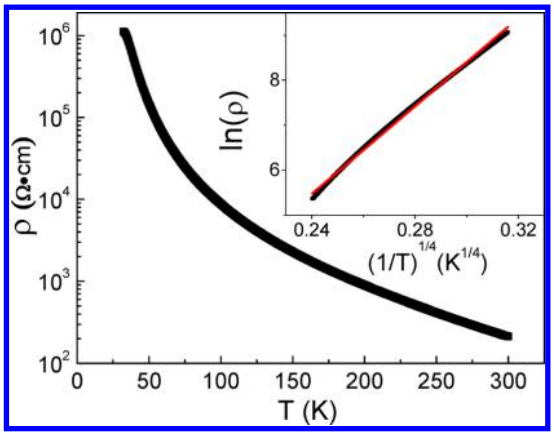

Figure 3. Temperature dependence of resistivity of $Pb_2Co_2O_7$. The inset shows the fitting result by the 3D Mott variable range hopping model between 250 and 300 K.

resistivity of $Pb_2Co_2O_7$ as a function of temperature. Since Pb^{4+} with a closed cell electronic configuration governs the *B* site, the compound exhibits electrical insulating behavior in the whole temperature region we measured, as featured by the increasing resistivity on cooling. Moreover, above 250 K, the temperature dependence of resistivity can be fitted on the basis of a 3D Mott variable range hopping model with the formula $\rho(T) = \rho_0 \exp(T_0/T)^{1/4}$, as shown in the inset of Figure 3, further revealing the insulating nature of $Pb_2Co_2O_7$ as expected from structural and charge state analysis.

The magnetism of $Pb_2Co_2O_7$ was studied by both dc and ac magnetization. As shown in Figure 4a, the dc zero-field-cooling (ZFC) and field-cooling (FC) magnetic susceptibility curves remarkably separate from each other at the critical temperature $T_f \approx 20$ K at 0.1 T. Moreover, with increasing magnetic field, T_f systematically shifts toward lower temperature, accompanied by the gradual reduction and broadening of the ZFC magnetic susceptibility cusp around T_f. Below T_f, the compound shows magnetic hysteresis but nonsaturated magnetization behavior (inset of Figure 4a). When the specific heat is measured, we do not find a visible anomaly near T_f (see the inset of Figure 4b). These features strongly suggest the occurrence of spin glassy behavior. The inverse magnetic susceptibility above 200 K can be well fitted on the basis of the Curie−Weiss law (see Figure 4b), producing the Weiss temperature $\Theta = -170.0$ K, which is much higher than the value of T_f. One therefore can calculate the frustration index to be $f = |\Theta|/T_f = 8.5$, indicating strong magnetic frustration. These results are in good agreement with the tetrahedral geometric frustration effects in a pyrochlore structure arising from the magnetic Co^{4+} ions. In addition, since Co^{4+} occupies only 40% of the *B* sites, the Co−Co magnetic interaction probably is competing between antiferromagnetism and ferromagnetism, which can also contribute to the spin glassy behavior.

DOI: 10.1021/acs.inorgchem.7b01646
Inorg. Chem. 2017, 56, 11676−11680

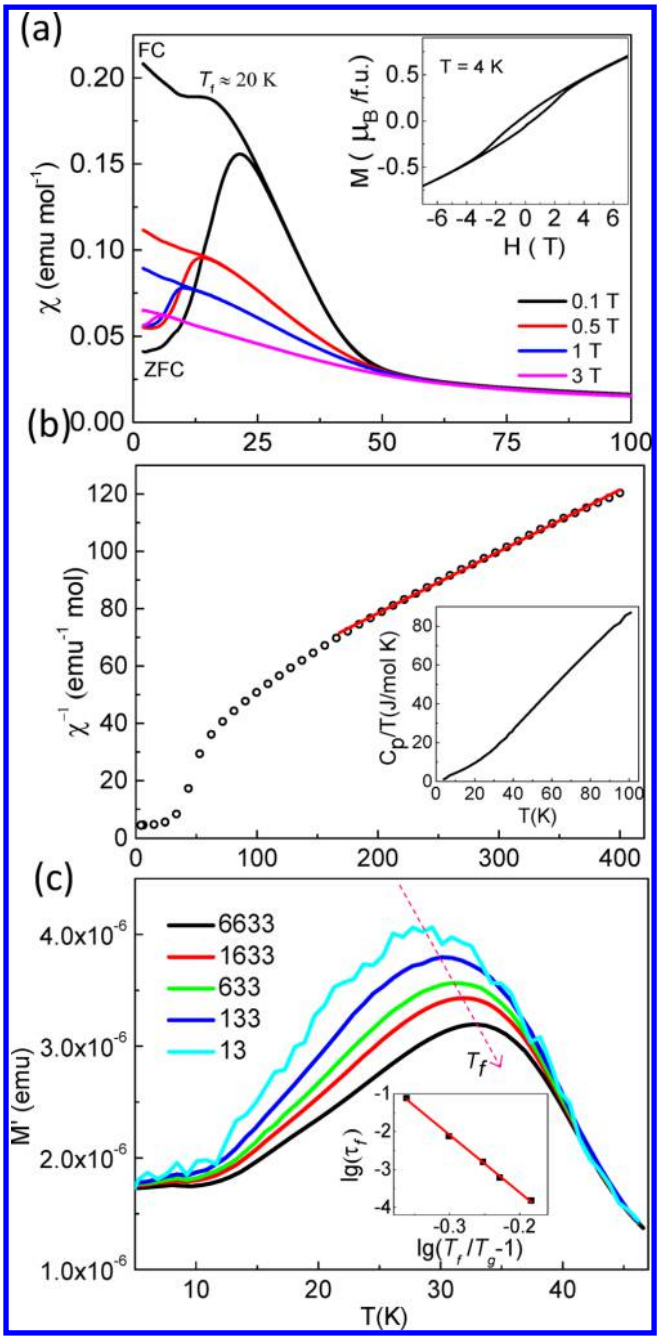

Figure 4. (a) Temperature-dependent dc magnetization measured at different magnetic fields. The inset shows the field dependence of isothermal magnetization measured at 4 K. (b) Temperature-dependent dc magnetization measured at H = 0.1 T. The solid line shows the Curie–Weiss fitting above 200 K. The inset shows specific heat data collected between 2 and 100 K. (c) Temperature-dependent ac magnetization. The inset shows the plot of log τ_f vs log$(T_f/T_g - 1)^{-zv}$ and the fitted result.

To further confirm the spin glassy nature of $Pb_2Co_2O_7$, ac magnetization was measured at different frequencies, as shown in Figure 4c. Obviously, the spin freezing temperature T_f increases with increasing frequency. This can be regarded as convincing evidence for the presence of spin glass because with increasing frequency the spin directions are less able to follow the oscillating field and therefore spin freezing occurs. Usually, the frequency dependence of T_f in spin glass can be described by the conventional critical slowing down behavior with the function $\tau_f = \tau_0(T_f/T_g - 1)^{-zv}$. Here $\tau_f = 1/f$ corresponds to the maximum relaxation time of the system at temperature T_f, τ_0 is the intrinsic relaxation time of the spin dynamics, T_g is the freezing temperature at f = 0, and zv is the dynamic exponent. Figure 4c shows the good fit of $Pb_2Co_2O_7$ using this function, yielding $\tau_0 = [2.26(3)] \times 10^{-7}$ s and zv = 15.19(2). Both values are comparable with the results found in other pyrochlore spin glassy systems,[5] further confirming the glassy magnetic behavior of $Pb_2Co_2O_7$ pyrochlore.

IV. CONCLUSIONS

The new oxide $Pb_2Co_2O_7$ has been prepared for the first time by using a high-pressure and high-temperature method. Synchrotron X-ray diffraction confirms that this compound is the first cobalt-based pyrochlore with space group $Fd\bar{3}m$. Rietveld structural analysis demonstrates a large mixed cation occupancy at both the A and B sites by about 40%. On the basis of the X-ray absorption spectroscopy results, the specific chemical composition and charge states can be assigned to be $(Co_{0.6}Pb_{0.4})_2^{3+}(Pb_{0.6}Co_{0.4})_2^{4+}O_7$, where low-spin Co^{3+} and average Pb^{3+} occupy the A site and Pb^{4+} and low-spin Co^{4+} occupies the B site with a 3:2 mol ratio. Since the distinct charge states of Pb and Co at different atomic sites have different ionic sizes, the A–B antisite disorder can be suppressed significantly. As a result, $Pb_2Co_2O_7$ exhibits electrical insulating behavior which follows the 3D Mott variable range hopping mechanism. In magnetism, the strong geometric frustration effects and the partial occupancy of magnetic Co^{4+} ions at the B site make the compound spin glassy, well in agreement with the conventional critical slowing down behavior.

AUTHOR INFORMATION

Corresponding Authors

*E-mail for M.A.: mazuma@msl.titech.ac.jp.
*E-mail for Y.L.: ywlong@iphy.ac.cn.

ORCID

Yunliang Soo: 0000-0002-1683-3141
Masaki Azuma: 0000-0002-8378-321X
Youwen Long: 0000-0002-8587-7818

Notes

The authors declare no competing financial interest.

ACKNOWLEDGMENTS

The authors thank L. X. Li for structural determination and fruitful discussions. This work was supported by the 973 Project of the Ministry of Science and Technology of China (Grant No. 2014CB921500), the National Natural Science Foundation of China (Grant Nos. 11574378, 51772324, and 61404052), and the Chinese Academy of Sciences (Grant Nos. QYZDB-SSW-SLH013, XDB07030300, YZ201555, and GJHZ1773). M. Azuma was supported by Kanagawa Institute of Industrial Science and Technology. Y. Long was partially supported by World Research Hub Initiative, Institute of Innovative Research, Tokyo Institute of Technology and Collaborative Research Projects, Laboratory for Materials and Structures, Tokyo Institute of Technology.

REFERENCES

(1) Yoshii, S.; Iikubo, S.; Kageyama, T.; Oda, K.; Kondo, Y.; Murata, K.; Sato, M. Anomalous Hall effect of pyrochlore molybdate $Nd_2Mo_2O_7$. *J. Phys. Soc. Jpn.* **2000**, *69*, 3777–3780.

DOI: 10.1021/acs.inorgchem.7b01646
Inorg. Chem. 2017, 56, 11676–11680

(2) Hanawa, M.; Muraoka, Y.; Tayama, T.; Sakakibara, T.; Yamaura, J.; Hiroi, Z. Superconductivity at 1 K in $Cd_2Re_2O_7$. *Phys. Rev. Lett.* **2001**, *87*, 187001.
(3) Shimakawa, Y.; Kubo, Y.; Manako, T. Giant magnetoresistance in $Tl_2Mn_2O_7$ with the pyrochlore structure. *Nature* **1996**, *379*, 53−55.
(4) Nakatsuji, S.; Machida, Y.; Maeno, Y.; Tayama, T.; Sakakibara, T.; van Duijn, J.; Balicas, L.; Millican, J. N.; Macaluso, R. T.; Chan, J. Y. Metallic Spin-Liquid Behavior of the Geometrically Frustrated Kondo Lattice $Pr_2Ir_2O_7$. *Phys. Rev. Lett.* **2006**, *96*, 087204.
(5) Gardner, J. S.; Gingras, M. J. P.; Greedan, J. E. Magnetic pyrochlore oxides. *Rev. Mod. Phys.* **2010**, *82*, 53−99.
(6) Long, Y. W.; Kaneko, Y.; Ishiwata, S.; Taguchi, Y.; Tokura, Y. Synthesis of cubic $SrCoO_3$ single crystal and its anisotropic magnetic and transport properties. *J. Phys.: Condens. Matter* **2011**, *23*, 245601.
(7) Long, Y. W.; Kaneko, Y.; Ishiwata, S.; Tokunaga, Y.; Matsuda, T.; Wadati, H.; Tanaka, Y.; Shin, S.; Tokura, Y.; Taguchi, Y. Evolution of magnetic phases in single crystals of $SrFe_{1-x}Co_xO_3$ solid solution. *Phys. Rev. B: Condens. Matter Mater. Phys.* **2012**, *86*, 064436.
(8) Jeen, H.; Choi, W. S.; Biegalski, M. D.; Folkman, C. M.; Tung, I. C.; Fong, D. D.; Freeland, J. W.; Shin, D.; Ohta, H.; Chisholm, M. F.; Lee, H. N. Reversible redox reactions in an epitaxially stabilized $SrCoO_x$ oxygen sponge. *Nat. Mater.* **2013**, *12*, 1057−1063.
(9) Cho, J.; Kim, Y. J.; Park, B. Novel $LiCoO_2$ Cathode Material with Al_2O_3 Coating for a Li Ion Cell. *Chem. Mater.* **2000**, *12*, 3788−3791.
(10) Yoo, S.; Jun, A.; Ju, Y. W.; Odkhuu, D.; Hyodo, J.; Jeong, H. Y.; Park, N.; Shin, J.; Ishihara, T.; Kim, G. Development of Double-Perovskite Compounds as Cathode Materials for Low-Temperature Solid Oxide Fuel Cells. *Angew. Chem., Int. Ed.* **2014**, *53*, 13064−13067.
(11) Maignan, A.; Martin, C.; Pelloquin, D.; Nguyen, N.; Raveau, B. Structural and magnetic studies of ordered oxygen-deficient perovskites $LnBaCo_2O_{5+\delta}$, closely related to the ″112″ structure. *J. Solid State Chem.* **1999**, *142*, 247−259.
(12) Choi, Y. J.; Yi, H. T.; Lee, S.; Huang, Q.; Kiryukhin, V.; Cheong, S. W. Ferroelectricity in an Ising Chain Magnet. *Phys. Rev. Lett.* **2008**, *100*, 047601.
(13) Kim, J. W.; Kamiya, Y.; Mun, E. D.; Jaime, M.; Harrison, N.; Thompson, J. D.; Kiryukhin, V.; Yi, V. H.; Oh, Y. S.; Cheong, S. W.; Batista, C. D.; Zapf, V. S. Multiferroicity with coexisting isotropic and anisotropic spins in $Ca_3Co_{2-x}Mn_xO_6$. *Phys. Rev. B: Condens. Matter Mater. Phys.* **2014**, *89*, 060404.
(14) Sawaguchi, E. Ferroelectricity versus Antiferroelectricity in the Solid Solutions of $PbZrO_3$ and $PbTiO_3$. *J. Phys. Soc. Jpn.* **1953**, *8*, 615−629.
(15) Shimada, T.; Wang, J.; Araki, Y.; Mrovec, M.; Elsässer, C.; Kitamura, T. Multiferroic Vacancies at Ferroelectric $PbTiO_3$ Surfaces. *Phys. Rev. Lett.* **2015**, *115*, 107202.
(16) Mani, B. K.; Chang, C. M.; Lisenkov, S.; Ponomareva, I. Critical Thickness for Antiferroelectricity in $PbZrO_3$. *Phys. Rev. Lett.* **2015**, *115*, 097601.
(17) Sakai, Y.; Yang, J. Y.; Yu, R. Z.; Hojo, H. J.; Yamada, I.; Miao, P.; Lee, S.; Torii, S.; Kamiyama, T.; Ležaić, M.; Bihlmayer, G.; Mizumaki, M.; Komiyama, J.; Mizokawa, T.; Yamamoto, H. J.; Nishikubo, T.; Hattori, Y.; Oka, K.; Yin, Y. Y.; Dai, J. H.; Li, W. M.; Ueda, S.; Aimi, A.; Mori, D.; Inaguma, Y.; Hu, Z. W.; Uozumi, T.; Jin, C. Q.; Long, Y. W.; Azuma, M. A-Site and B-Site Charge Orderings in an s-d Level Controlled Perovskite Oxide $PbCoO_3$. *J. Am. Chem. Soc.* **2017**, *139*, 4574−4581.
(18) Rodŕıguez-Carvajal, J. Recent advances in magnetic structure determination by neutron power diffraction. *Phys. B* **1993**, *192*, 55−69.
(19) Gregg, D. J.; Zhang, Z. M.; Thorogood, Z. J.; Kennedy, B. J.; Kimpton, J. A.; Griffiths, G. J.; Guagliardo, P. R.; Lumpkin, G. R.; Vance, E. R. Cation antisite disorder in uranium-doped gadolinium zirconate Pyrochlores. *J. Nucl. Mater.* **2014**, *452*, 474−478.
(20) Lin, H.-J.; Chin, Y. Y.; Hu, Z. W.; Shu, G. J.; Chou, F. C.; Ohta, H.; Yoshimura, K.; Hébert, S.; Maignan, A.; Tanaka, A.; Tjeng, L. H.; Chen, C. T. Local orbital occupation and energy levels of Co in Na_xCoO_2: A soft x-ray absorption study. *Phys. Rev. B: Condens. Matter Mater. Phys.* **2010**, *81*, 115138.
(21) Ohta, H.; Yoshimura, K.; Hu, Z. W.; Chin, Y. Y.; Lin, H.-J.; Hsieh, H. H.; Chen, C. T.; Tjeng, L. H. Determination of the Co Valence in Bilayer Hydrated Superconducting Na_xCoO_2 •yH_2O by Soft X-Ray Absorption Spectroscopy. *Phys. Rev. Lett.* **2011**, *107*, 066404.
(22) Izumi, Y.; Kiyotaki, F.; Minato, T.; Masih, D.; Seida, Y. Monitoring trace amounts of lead and arsenic adsorption by X-ray absorption fine structure combined with fluorescence spectrometry. *Phys. Scr.* **2005**, *115*, 933−935.
(23) Liang, G.; Yao, G.; Zhou, Q.; Katz, S. D. X-ray absorption near-edge structure study of $Bi_{2-x}Pb_xSr_2(Sm_{0.85}Ce_{0.15})_2Cu_2O_{10+y}$. *Phys. C* **2005**, *424*, 107−115.

DOI: 10.1021/acs.inorgchem.7b01646
Inorg. Chem. 2017, 56, 11676−11680